Supplementary Materials for

Chiral Nematic Cellulose / Gold Nanoparticle Composites from Mesoporous Photonic Cellulose

Maik Schlesinger,[a] Michael Giese,[a] Lina K. Blusch,[a] Wadood Y. Hamad[b] and Mark J. MacLachlan*[,a]

Experimental section

Materials and Instrumentation

All compounds were used as received without any further purification. Aqueous suspensions of cellulose nanocrystals (CNCs) were supplied from CelluForce, Inc. in a neutral form (CNC-Na: 5%, pH = 6.9), which were obtained by a previously described procedure.[1]

Thermogravimetric analysis was performed with a Pyris 6 (PerkinElmer) under air with a heating rate of 10 °C min^{-1}. CD spectroscopy was recorded on a J-710 spectropolarimeter (JASCO) by attaching the films on quartz slides perpendicular to the beam path. Some representative films were additionally turned in order to exclude linear effects. UV-Vis/NIR spectra were recorded on a Cary 5000 UV-Vis/NIR spectrophotometer by using the same procedure as that used for CD measurements. Nitrogen adsorption isotherms were conducted at 77 K using a Micromeritics ASAP 2020 analyzer. Pore-size distributions were obtained from the adsorption branches using the Barrett-Joyner-Halenda (BJH) method. Electron microscopy studies were performed on a Hitachi S4700 (SEM) with sputter-coated samples (3.0 nm of gold/palladium 60/40) and on a Hitachi H7600 electron microscope (TEM). The nanoparticle size distributions were calculated from TEM images using the LINCE (linear intercept) software (TU Darmstadt). The size distributions are based on counts of 150-166 particles in each case from several TEM images. The quoted errors represent standard deviations in the particle size distributions. Powder X-ray diffraction studies were carried out on a D8 Advance (Bruker) using Cu-K_α irradiation and a NaI scintillation detector. The deconvolution of the peaks of the diffraction patterns was done by the use of DIFFRACplus TOPAS software (Bruker-AXS) on the basis of the Rietveld refinements.[2] The degree of crystallinity X_c (the fraction in weight occupied by the crystallites) was calculated using Ruland's theoretical approach.[3] Critical point drying with supercritical CO_2 was done on an autosamdry-815 critical point dryer (Tousimis Research Corporation).

Synthesis of mesoporous photonic cellulose (MPC)

The synthesis of MPC was performed according to a recently published procedure, which includes drying with supercritical CO_2.[4] Briefly, MPC was synthesized by mixing 5 mL of a CNC suspension (CNC-Na, pH 6.9, 3 wt%) with 1 mL of a urea-formaldehyde (UF) precursor, which was prepared from 2 g urea, 10 g of formaldehyde and one drop of HCl (37%). After drying the mixture on cellulose acetate (5 cm diameter) the resulting film was cured at 120°C in an oven, the polymer was removed by treatment with an aqueous KOH solution (30 wt%, 200 mL) at 75 °C for 16 h, and, finally, washed and dried with supercritical CO_2.

Synthesis of mesoporous photonic cellulose with a distorted chiral nematic structure (MPCII)

MPCII was obtained by using the same procedure than for MPC whereas 10 drops of HCl (37%) were added during mixing of the CNCs suspension with the UF precursor.

Functionalization with gold nanoparticles

10 mg of MPC were soaked in 5 mL of 5 mM, 10 mM or 100 mM aqueous solutions of $HAuCl_4$ for 1 h. Afterwards the films were washed several times with water and ethanol and dried under ambient conditions. To complete nanoparticle formation, the films were soaked in 10 mL of a freshly prepared 200 mM $NaBH_4$(aq) solution for 1 h, washed several times with water and ethanol, and dried under ambient conditions.

Figures

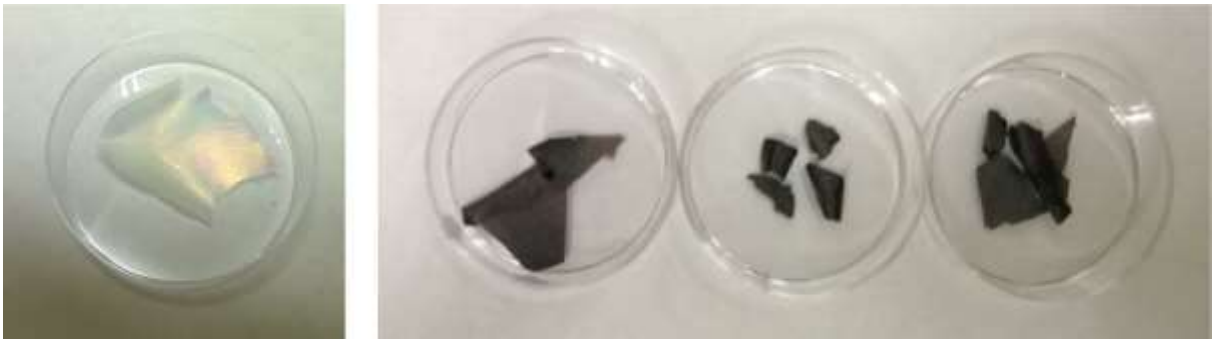

Figure S1. Photographs of unloaded MPC (left image) and the gold nanoparticle-loaded films (right image): **MPC-Au-5** (left), **MPC-Au-10** (middle) and **MPC-Au-100** (right).

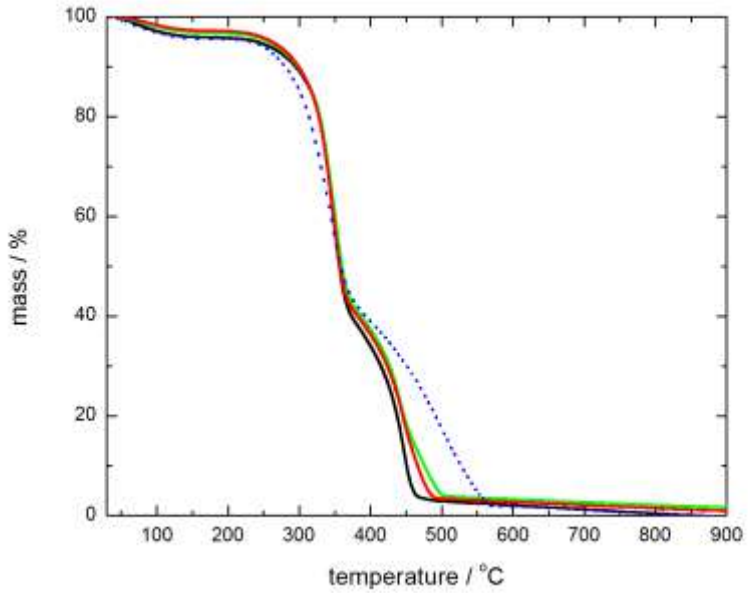

Figure S2. TG curves of unloaded MPC (blue; dotted line), **MPC-Au-5** (black; solid line), **MPC-Au-10** (red; solid line) and **MPC-Au-100** (green; solid line).

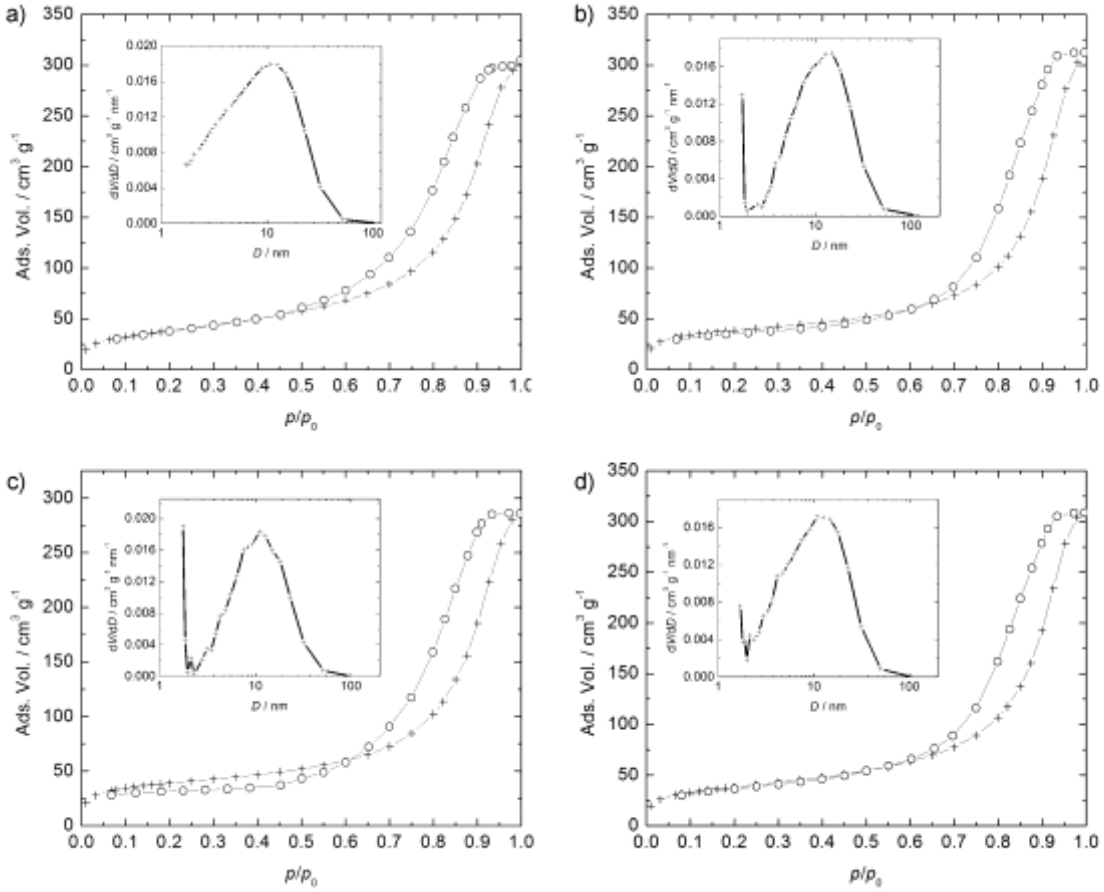

Figure S3. Isothermal N_2 adsorptions of unloaded **MPC** (a), **MPC-Au-5** (b), **MPC-Au-10** (c) and **MPC-Au-100** (d) after drying with supercritical carbon dioxide. Inset: Corresponding BJH pore-size distributions calculated from the adsorption branch of the isotherm.

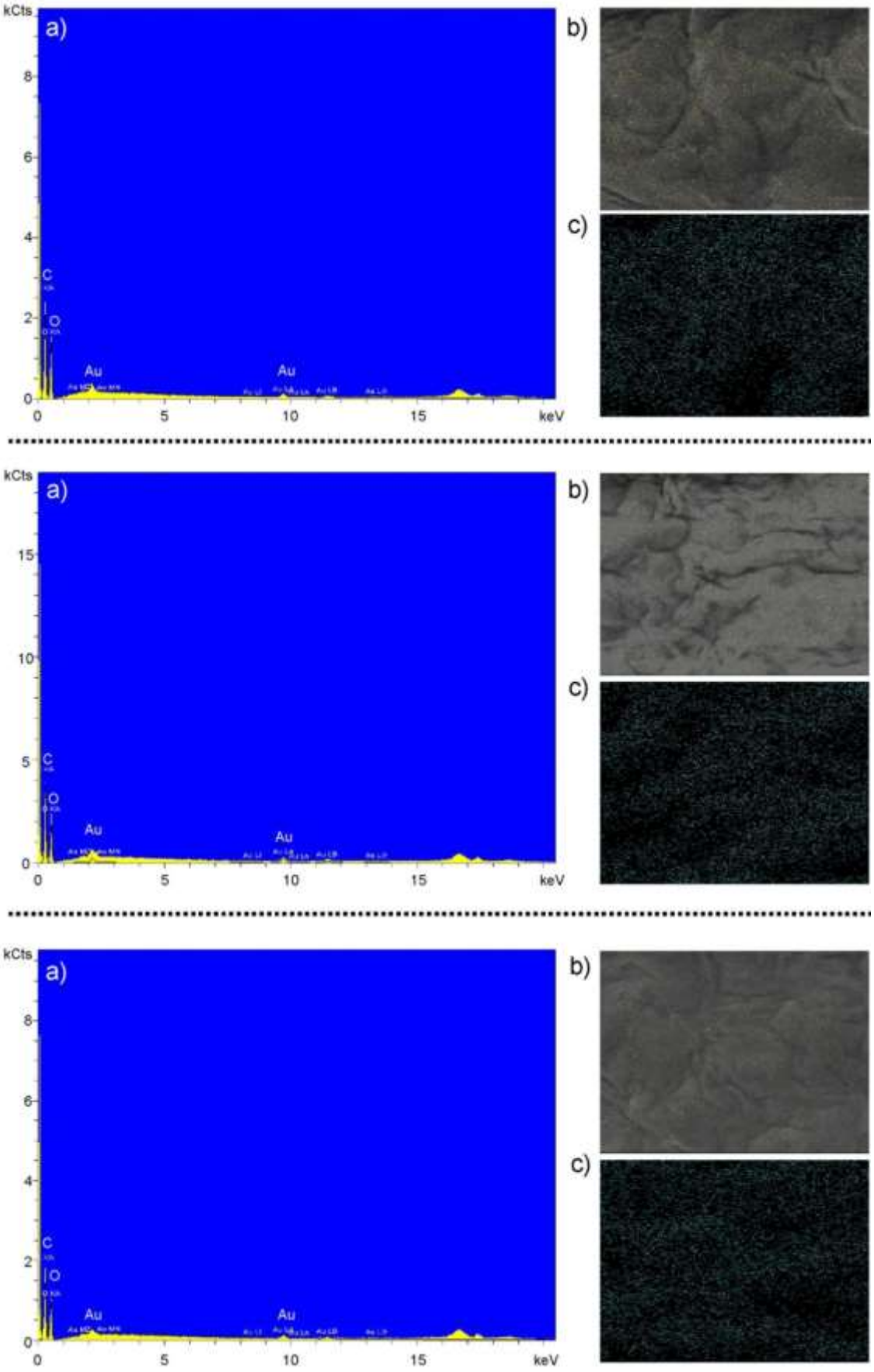

Figure S4. EDX spectra (a), EDX mapping combined with SEM image (b) and EDX mapping for gold (c) of of **MPC-Au-5** (top), **MPC-Au-10** (middle) and **MPC-Au-100** (bottom).

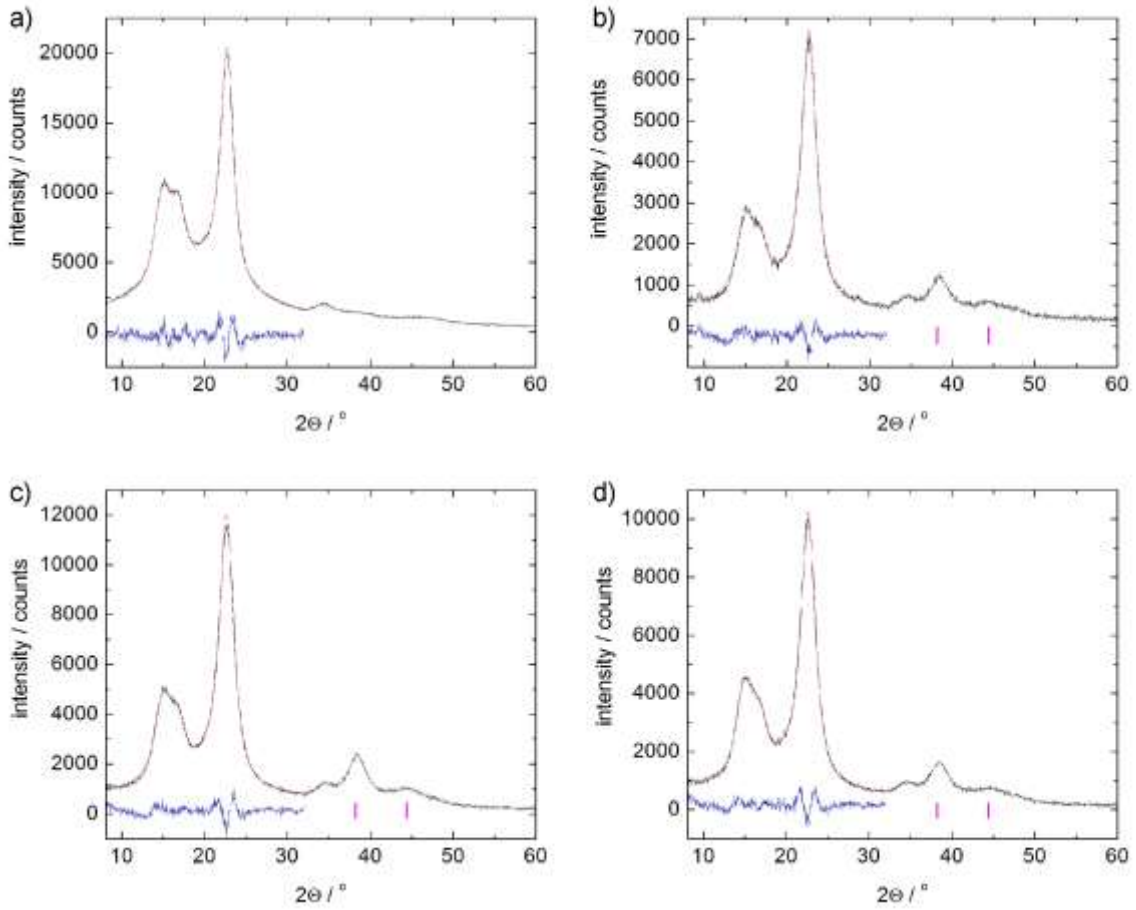

Figure S5. Powder X-ray diffraction patterns (black lines) of MPC (a), **MPC-Au-5** (b), **MPC-Au-10** (c) and **MPC-Au-100** (d). The diffraction patterns are resolved between 8° - 32° 2θ into crystalline peaks and amorphous background (this region was used as there is no interference with the diffraction peaks of Au NPs (magenta; PDF 03-065-2870)). The refinement was done using the Ruland-Rietveld analytical approach of the crystal structure of cellulose Iα (CCDC 792796; red lines). The degree of crystallinity was determined to be ~62% (MPC), ~71% (**MPC-Au-5**), ~72% (**MPC-Au-10**) and ~74% (**MPC-Au-100**).

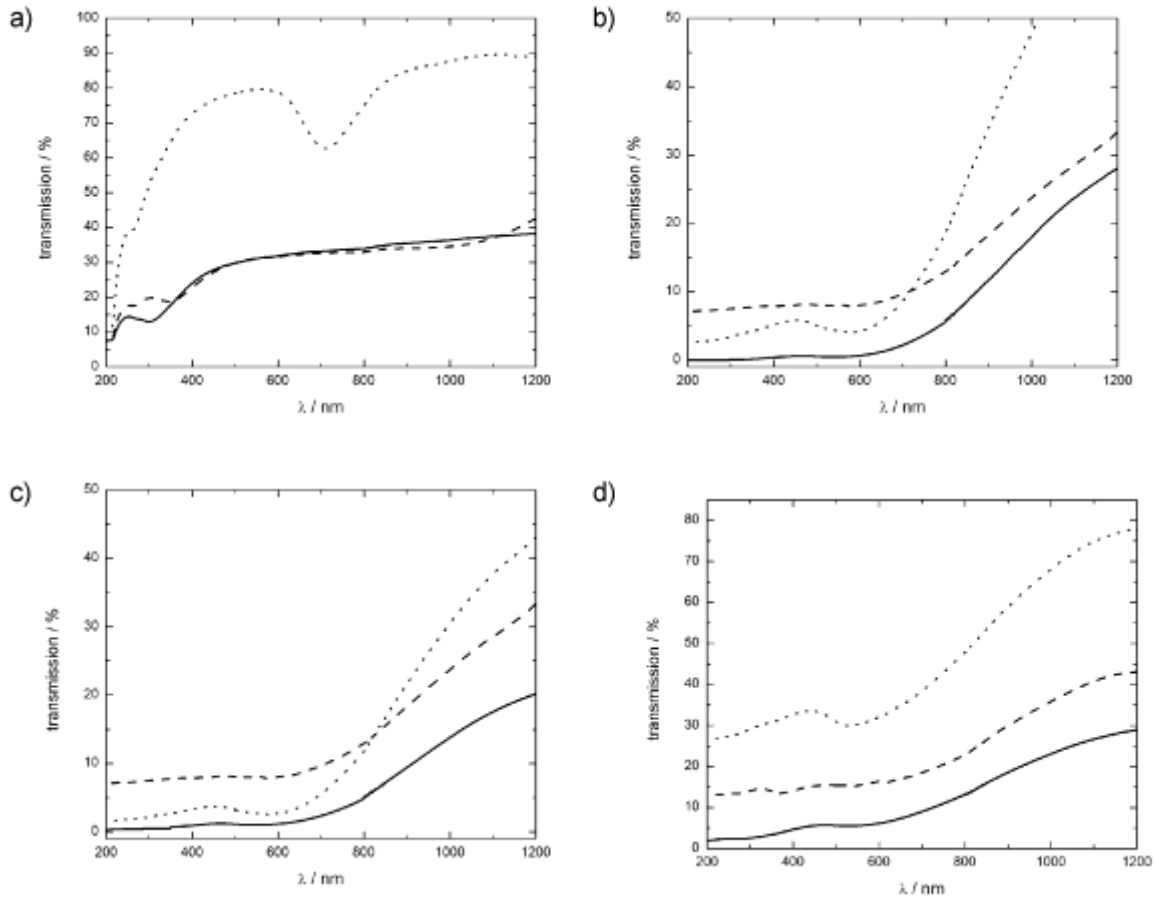

Figure S6. UV/Vis spectra of unloaded MPC (a), **MPC-Au-5** (b), **MPC-Au-10** (c) and **MPC-Au-100** (d) in dried state (solid lines) and soaked in ethanol (dashed lines) or water (dotted lines).

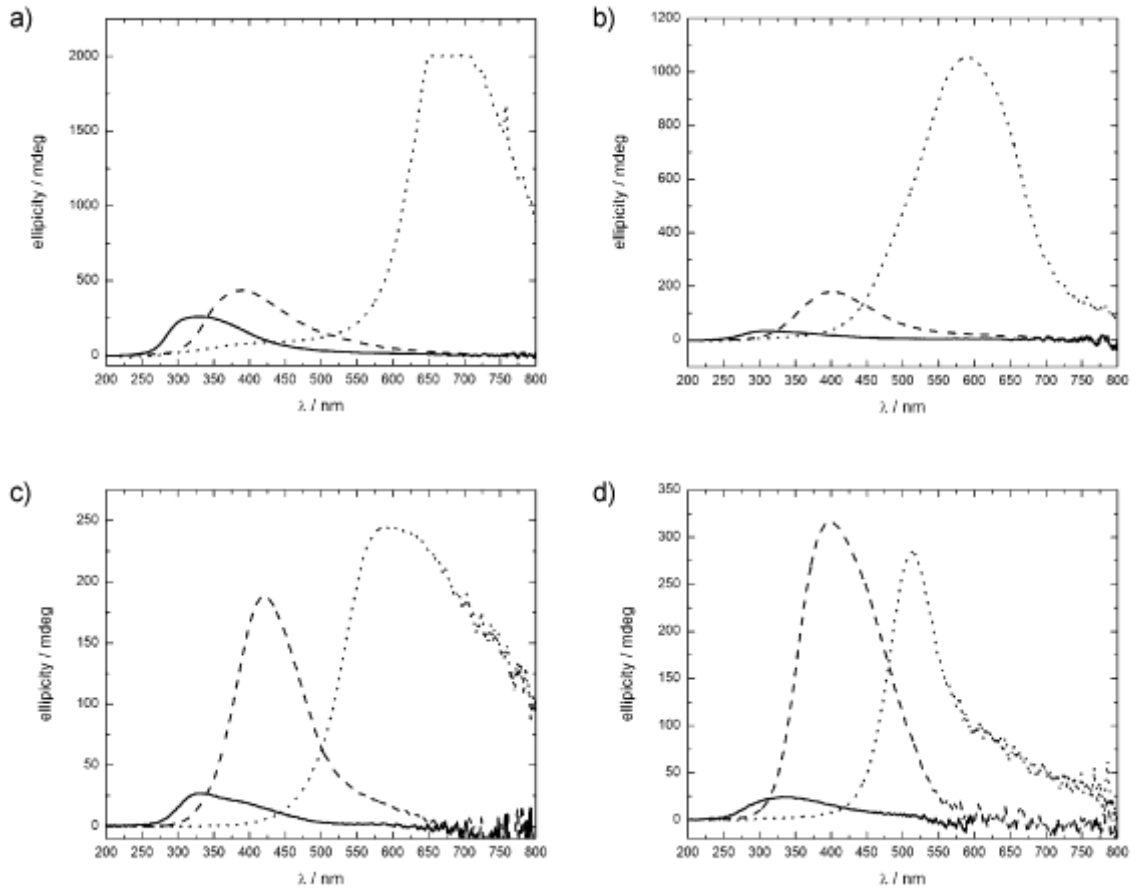

Figure S7. CD spectra of unloaded MPC (a), **MPC-Au-5** (b), **MPC-Au-10** (c) and **MPC-Au-100** (d) in dried state (solid lines) and soaked in ethanol (dashed lines) or water (dotted lines).

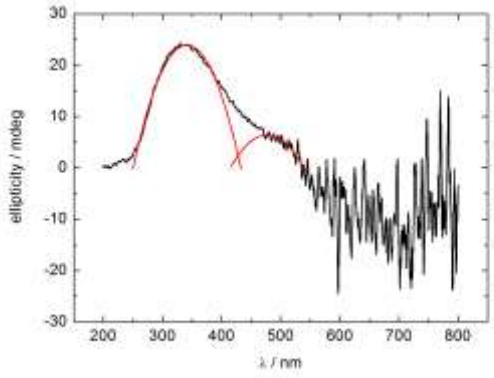

Figure S8. CD spectra of dry **MPC-Au-100** (black) including fitted functions (red) to clarify the existence of two separate CD signals.

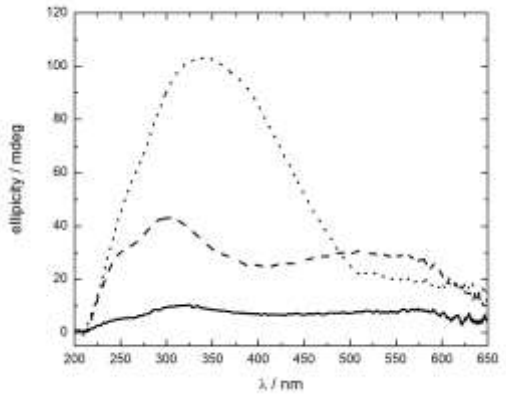

Figure S9. CD spectra of dry **MPCII-Au-100** (solid lines) and **MPCII-Au-100** soaked in ethanol (dashed lines) or water (dotted lines).

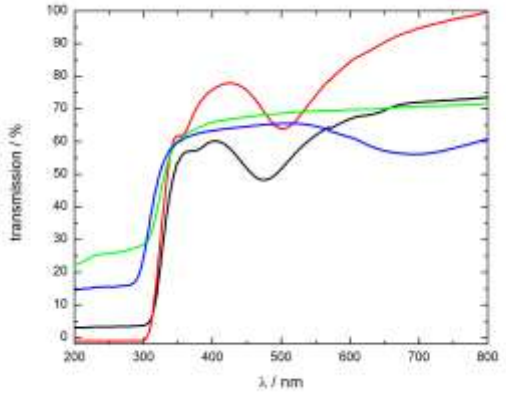

Figure S10. UV/Vis spectra of **MPC-Au-100** soaked in 2-mercaptoethanol (black) or water (red) and unloaded MPC soaked in 2-mercaptoethanol (green) or water (blue). The UV/Vis reflection band of unloaded MPC soaked in 2-mercaptoethanol (green) is shifted to 1193 nm and is omitted for clarity.

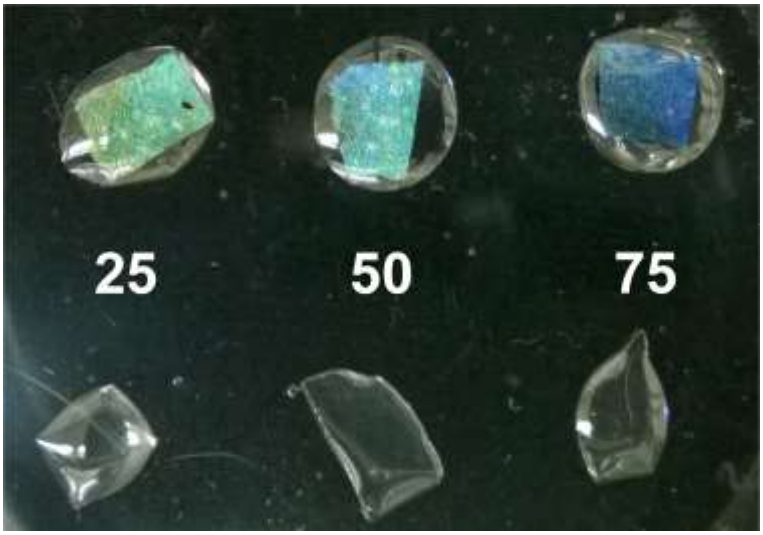

Figure S11. Photographs of **MPC-Au-100** (top) and unloaded MPC (bottom) after addition of an aqueous solution of 2-mercaptoethanol (**25**: 25 vol% 2-mercaptoethanol; **50**: 50 vol% 2-mercaptoethanol; **75**: 75 vol% 2-mercaptoethanol).

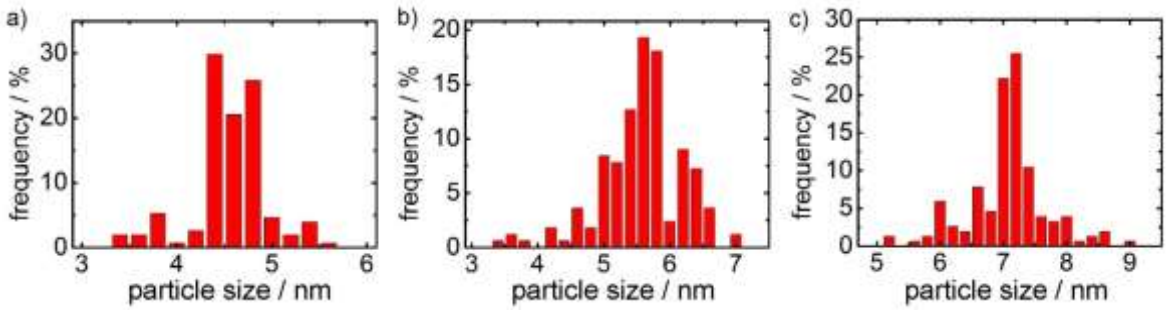

Figure S12. Particle size distributions of the Au NPs in a) **MPC-Au-5**, b) **MPC-Au-10** and c) **MPC-Au-100**. 150, 166, and 153 particles were counted for **MPC-Au-5**, **MPC-Au-10** and **MPC-Au-100**, respectively.

Tables

Table S1. Summary of determined BET surface areas, BJH pore size distributions and average pore volumes of unloaded MPC, **MPC-Au-5**, **MPC-Au-10** and **MPC-Au-100**.

	Unloaded MPC	**MPC-Au-5**	**MPC-Au-10**	**MPC-Au-100**
BET surface area (m^2 g^{-1})	138	130	132	133
BJH pore size (nm)	13.7	14.9	13.4	14.4
Pore volume (cm^3 g^{-1})	0.47	0.48	0.44	0.48

References

1 K. E. Shopsowitz, H. Qi, W. Y. Hamad and M. J. MacLachlan, *Nature*, 2010, **468**, 422-425.

2 H. M. Rietveld, *J. Appl. Crystallogr.*, 1969, **2**, 65-71.

3 W. Ruland, *Acta Cryst.*, 1961, **14**, 1180-1185.

4 M. Giese, L. K. Blusch, M. K. Khan, W. Y. Hamad and M. J. MacLachlan, *Angew. Chem. Int. Ed.*, 2014, **53**, 8880-8884.